E-13 ON SOME THEORETICAL AND EXPERIMENTAL INVESTIGATIONS OF HIGH SPEED PLASTIC DEFORMATION

K.Kawata[1], S.Fukui[1]. and J.Seino[2]

Abstract

High speed tension of a bar of finite length is analyzed using characteristics basing upon plastic wave theory. The solution of the relation of breaking strain ε_b versus tensile velocity V_1 is derived in an explicit form. Next, the relation is determined experimentally for several metals, in the velocity range up to 200 m/s(strain rate $\dot{\varepsilon} = 4.4 \times 10^3/s$). It is found that ε_b in high speed tension is larger than statical ε_b for some metals, but smaller for the others. Some remarkable correlation may be observed between the variation of ε_b with increasing V_1 and crystal structure for tested metals.

Introduction

It is found that ε_b in high speed tension is larger than statical ε_b for some metals, but smaller for the others, by our preliminary experiment. To clarify the relation between the tendencies and crystal structures of metals, a series of high speed tension test is carried out. A newly developed high speed loading machine using explosion pressure of low explosives which may realize tensile speeds up to 200 m/s is used. To compare the experimental relation of ε_b versus V_1 with the corresponding theoretical relation, the latter is derived basing upon plastic wave theory. The obtained theoretical relations are never flat, but of saw-teeth, and seem to be useful to explain several tendencies in the experimental relations, especially scattering of ε_b values.

Theoretical Analysis of the Plastic Wave Propagation in High Speed Tension of a Bar of Finite Length

The equation of motion for an element initially of length dx, of a bar under tension, is

$$A\rho\, dx \frac{\partial^2 u}{\partial t^2} = A \frac{\partial \sigma}{\partial x} dx \tag{1}$$

That is

$$c^2 \frac{\partial^2 u}{\partial x^2} = \frac{\partial^2 u}{\partial t^2} \quad (2), \qquad c^2 = \frac{1}{\rho} \cdot \frac{d\sigma}{d\varepsilon} \quad (3)$$

1 Institute of Space and Aeronautical Science, University of Tokyo, Professor

2 Shinshu University, Assistant Professor

where x: Lagrange coordinate along initially unstrained bar
u: displacement of a section
σ: nominal stress, force per unit initial cross-sectional area
ε: strain $= \partial u/\partial x$
A: initial cross-sectional area of bar
t: time
ρ: density of material unstrained.

Elasto-plastic material having a linear stress-strain relation in the plastic range as shown in Fig.1 and (4) is assumed.

$$\left.\begin{array}{ll} 0 \leqq \sigma \leqq \sigma_y & \varepsilon = \sigma/E \\ \sigma_y \leqq \sigma & \varepsilon = \varepsilon_y + (\sigma - \sigma_y)/E_p \end{array}\right\} \qquad (4)$$

The propagation velocities of waves are obtained as

$$\left.\begin{array}{ll} c^2 = c_0^2 = E/\rho & \text{for the elastic range} \\ c^2 = E_p/\rho & \text{for the plastic range} \end{array}\right\} \qquad (5)$$

The characteristic lines in (x,t) plane for (2) are

$$dx/dt = \pm c \qquad (6)$$

The shock conditions are

$$(\rho c v + \sigma)_1 = (\rho c v + \sigma)_2 \qquad (7)$$

for waves travelling in the positive direction, and

$$(\rho c v - \sigma)_1 = (\rho c v - \sigma)_2 \qquad (8)$$

for waves travelling in the negative direction, where points 1 and 2 are just ahead and behind of a stress wave front, and c is the absolute value of the velocity of wave propagation, though stress σ and particle velocity v may take positive or negative values. Application of (7) and (8) enables to determine stress and particle velocity distributions in the (x,t) plane.

We consider a bar extending from x=0 to x=l and assume that the free end point at x=0 is put into motion instantaneously at t=0 with the constant velocity $v = -V_1$ whereas the other end x=l is fixed as shown in Fig.2. V_1 is assumed large enough to cause the stress σ not smaller than σ_y at x=0, t=0. In this case, (x,t) diagram is as shown in Fig.3. If E is assumed to approach to infinity as a special case, Fig.3 reduces to Fig.4

This simple case is considered first. If stress and particle velocity are put equal to σ_n and v_n respectively in the region n, (σ_n, v_n) are determined generally as

$$\sigma_y + n\rho c V_1, \; -V_1 \; \left(1 + (-1)^{n+1}\right)/2 \qquad (9)$$

The relation of breaking strain versus tensile velocity V_1 may be derived using (9). If we assume breaking will occur instantaneously, where the condition:

$$\sigma_y + n\rho c V_1 \geqq \sigma_m > \sigma_y + (n-1)\rho c V_1 \qquad (10)$$

n: integer not smaller than 0

holds, breaking occurs at t=(n-1)l/c, and x=l if n is even, or x=0 if n is odd, and

$$\varepsilon_b = (n-1)\rho c V_1/E_p = (n-1)(V_1/V_{cr})\cdot \varepsilon_m \qquad (11)$$

where $V_{cr} = (\sigma_m - \sigma_y)/\rho c$ is the critical impact velocity for a bar of finite length and coincides with the one calculated for a bar of semi-infinite length.

The condition (10) can be written in the form:

$$V_{cr}/(n-1) > V_1 \geqq V_{cr}/n \qquad (12)$$

The plot of the relation of ε_b versus V_1 is obtained as shown in Fig.5. That is, the breaking strain ε_b of a bar of finite length in high speed tension is not always equal to the static breaking strain ε_m.

When E is not infinity, the stress σ_i and the particle velocity V_i for each region i are determined from Fig.3 as follows:

$$\begin{array}{ll} \text{region } 0: & \{\,0,\; 0\,\} \\ \text{region } 1: & \{\,\sigma_y,\; -\sigma_y/\rho c_0\,\} \\ \text{region } 2: & \{\,\sigma = (1 - c/c_0)\sigma_y + \rho c V_1,\; -V_1 = -\left(\frac{\sigma_y}{\rho c_0} + \frac{\sigma - \sigma_y}{\rho c}\right)\} \\ \text{region } 3: & \{\,(1 + c/c_0)\sigma_y,\; 0\,\} \end{array} \qquad \begin{array}{l}(13)\\(14)\\(15)\\(16)\end{array}$$

Generally,

$$\sigma_{a+3} - \sigma_a = \sigma + \frac{c}{c_0}\sigma_y - \sigma_y = \rho c V_1 = \text{Const.} \qquad (17)$$

where, a is integer larger than 0.

If we assume breaking will occur instantaneously, where the condition:

$$\sigma_i \geqq \sigma_m \qquad (18)$$

is satisfied for the first time, the breaking points may be A,B,C,D,E andF F. Their coordinates and abscissae are shown in Table 1. The residual strain distribution after breaking is not uniform and the mean value is defined as

$$\varepsilon = X\varepsilon_1 + (1-X)\varepsilon_2 \qquad (19)$$

The values of X (Fig.6) for each breaking point are obtained as shown in Table 2, considering the progress of stress waves before meeting with unloading wave after breaking.

For the region of V_1 where $\sigma_2 \geqq \sigma_3$, that is, $V_1 \geqq 2\sigma_y/\rho c_0$ holds, the relation of mean residual strain after breaking ε_b versus V_1 is obtained as follows:

region 2: When

$$\sigma_2 = (1 - c/c_0)\sigma_y + \rho c V_1 \geqq \sigma_m \qquad (20)$$

holds, breaking occurs at point 0 and

$$\varepsilon_b = 0 \qquad (21)$$

Because the condition (20) may be written in the form:

$$V_1 \geqq \sigma_y/\rho c_0 + (\sigma_m - \sigma_y)/\rho c \qquad (22)$$

the critical impact velocity is

$$V_{cr} = \sigma_y/\rho c_0 + (\sigma_m - \sigma_y)/\rho c \qquad (23)$$

region 4:

$$V_{cr} > V_1 \geqq V_{cr} - \sigma_y/\rho c_0 \quad \varepsilon_b = \tfrac{1}{2}(1/E_p - 1/E)\{-2(c/c_0)^2\sigma_y + (1 + c/c_0)\rho c V_1\} \qquad (24)$$

By the same process,

$$\begin{array}{lll} V_{cr} - \sigma_y/\rho c_0 > V_1 \geqq \frac{1}{2}V_{cr} & \varepsilon_b = (1/E_p - 1/E)\rho c V_1 & (25) \\ \frac{1}{2}V_{cr} > V_1 \geqq \frac{1}{2}(V_{cr} - \sigma_y/\rho c_0) & \varepsilon_b = \frac{1}{2}(1/E_p - 1/E)\{-2(c/c_0)^2\sigma_y + (3 + c/c_0)\rho c V_1\} & (26) \\ \frac{1}{2}(V_{cr} - \sigma_y/\rho c_0) > V_1 \geqq \frac{1}{3}V_{cr} & \varepsilon_b = (1/E_p - 1/E)\,2\rho c V_1 & (27) \\ \frac{1}{3}V_{cr} > V_1 \geqq \frac{1}{3}(V_{cr} - \sigma_y/\rho c_0) & \varepsilon_b = \frac{1}{2}(1/E_p - 1/E)\{-2(c/c_0)^2\sigma_y + (5 + c/c_0)\rho c V_1\} & (28) \\ \frac{1}{3}(V_{cr} - \sigma_y/\rho c_0) > V_1 \geqq \frac{1}{4}V_{cr} & \varepsilon_b = (1/E_p - 1/E)\,3\rho c V_1 & (29) \end{array}$$

and so on. The plot of the relation of ε_b versus V_1 is of saw-teeth, as shown in an example, Fig.7, for which the numerical constants are,

$E = 2\text{x}10^4$ kg/mm^2, $E_p = 2\text{x}10^2$ kg/mm^2, $\sigma_y = 40$ kg/mm^2, $\sigma_m = 80$ kg/mm^2,
$\varepsilon_y = 0.002$, $\varepsilon_m = 0.202$, $\rho = 8\text{x}10^{-3}$ g.cm^{-4}.s^2, $c_0 = 5\text{x}10^3$ m/s,
$c = 5\text{x}10^2$ m/s, $\rho c V_1 = 0.40\ V_1$ kg/mm^2 (V_1 : m/s)

High Speed Tension Test of Several Metals

A high speed tension testing machine applying the explosion pressure of low explosives is developed. In the testing machine, high speed tension is given to the specimen through a striking jaw from the projectile ejected by the explosion pressure. The actual tensile speed of test specimen is smaller than the projectile speed, because the rigidity of load-introducing jaw is not infinity. The tensile speed is measured by means of a ultra high speed camera MLD-3(framing speed is ranging up to 200, 000 frames per second) or an electronic counter. In the present state actual tensile speed is ranging up to 200 m/s. The testing machine and accessories are shown in Figs.8 and 9. Main dimensions of test specimens are as follows: Total length:108 mm, and for central measuring part of uniform width: length: 45 mm, width: 10 mm, thickness: about 1 mm. ε_b is measured by means of parallel grids marked on the measuring part in the direction perpendicular to the direction of tension with intervals of 2 mm. Test materials are 99.5% Al(2S), 99.99% Al, 2024C-0 Al alloy, SPC-1 mild steel, 18-8 stainless steel and ST-60 Ti. Uniaxial tensile test are carried out in the velocity range from 0 to 200 m/s, that is, the strain rate range from 0 to about 4.4×10^3/s.

The relations of ε_b versus V_1 obtained experimentally are shown in Figs.10 and 11. Following results are observed.

(1) For 2S-0 Al, 2024C-0 Al alloy and 18-8 stainless steel, ε_b in high speed tension is larger than the static ones, in a wide range of V_1.

(2) For SPC-1 mild steel and ST-60 Ti, ε_b decreases with increasing V_1 in general tendency.

(3) Pure Al are studied in more detail(Fig.11). Test materials are 99.5% Al(2S) and 99.99% Al, in hard(as roll) and annealed(340± 10°C, 2~3 $\times 10^{-5}$ mm Hg, 18 hr) conditions. For 99.5% Al, in both conditions, ε_b in high speed tension is larger than the static ones. For 99.99% Al, it increases in hard condition, but decreases in annealed condition.

(4) For metals of face centred cubic lattice, ε_b in high speed tension is generally larger than the static ones in the velocity range above mentioned, except annealed 99.99% Al of very coarse grain. For metal of hexagonal close packed lattice, ε_b decreases with increasing V_1. For metal of body centred cubic lattice, a preliminary experiment on 6/4 brass is made also, in which ε_b increases with increasing V_1. So, for metals of b.c.c. lattice there are two tendencies of decreasing (SPC-1 mild steel) and increasing (6/4 brass) with increasing V_1. The universality of these remarkable correlations between the variation of ε_b with increasing V_1 and crystal structure should be studied further in a wider selection of materials.

(5) In comparison with the theoretical results, following points may be pointed out.

(i) The values of critical impact velocity basing upon the measured statical stress-strain relations are shown in Table 3. For these specimens, breaking elongation ε_b keep rather large values at some velocity range higher than V_{cr}.

(ii) Considerable portion of scattering observed in the measured relation of ε_b versus V_1 may be an essential behaviour as shown in the saw-teeth theoretical relation.

(iii) Some part of apparent decreasing of ε_b with increasing V_1 may be attributed to the theoretical behaviour. So, for SPC-1 mild steel and ST-60 Ti, ε_m in high speed tension is expected not so decreased than statical ε_m. For the materials that showed increasing tendency of ε_b with increasing V_1, ε_m in high speed tension shall be considerably larger than statical ε_m.

References

(1)Th. von Karman, P.E.Duwez: J.Appl.Phys., 21(1950), 987.
G.I.Taylor: J.Inst.Civil Engrs(London), 26(1946), 486.
H.A.Rakhmatulin: Priklad. Math. Mekh., 11(1947), 379.

(2)Th. von Karman, H.F.Bohnenblust, D.H.Hyers: NDRC Report A-103(OSRD 946)(1942).

(3)K.Kawata, S.Fukui, J.Seino: Aeronautical Res. Inst., Univ. of Tokyo, Report No.389(1964), 165.

(4)M.Manjoine, A.Nadai: Proc. ASTM, 40(1940), 822.
D.S.Clark, D.S.Wood: Trans. ASTM, 42(1950), 45.
D.S.Clark: Trans. ASM, 46(1954), 34.
T.Tsumura, S.Sakui, K.Okamoto, T.Nakamura, et al.: Proc. Third Japan Congress on Testing Materials(1960), 95.
F.E.Hauser, J.A.Simmons, J.E.Dorn: Response of Metals to High Velocity Deformation, Interscience, (1961), 93.
J.Harding, E.O.Wood, J.D.Campbell: J.Mech.Engg.Sci., 2(1960), 88; Response of Metals to High Velocity Deformation, Interscience, (1961), 51.

Table 1. Breaking point

breaking point	x	t
A	l	l/c_0
B	$\frac{l}{2}(1+\frac{c}{c_0})$	$\frac{l}{2}\cdot\frac{c+c_0}{cc_0}$
C	l	l/c
D	0	$\frac{l}{c_0}+\frac{l}{c}$
E	$\frac{l}{2}(1-\frac{c}{c_0})$	$\frac{l}{2}(\frac{3}{c}+\frac{1}{c_0})$
F	0	$2l/c$

Table 2. The values of X

breaking point	X
A	$2c/(c+c_0)$
B	$\frac{1}{2}(1+\frac{c}{c_0})$
C	0
D	$(c_0-c)/(c+c_0)$
E	$\frac{1}{2}(1-\frac{c}{c_0})$
F	1

Table 3. Critical impact velocity calculated basing upon measured statical stress-strain relation

material	2S-0 Al	2024C-0 Al alloy	SPC-1 mild steel	18-8 stainless steel	ST-60 Ti
V_{cr} (m/s)	49.7	63.1	30.0	152.3	61.8

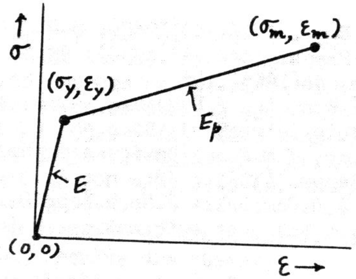

Fig.1 Elastic-linearly work hardening material property. σ_y is yield stress. It is assumed breaking occurs instantaneously when stress reaches to σ_m. E and Ep are the tangents.

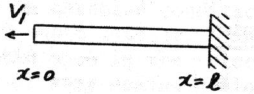

Fig.2 High speed tension of a bar of length l.

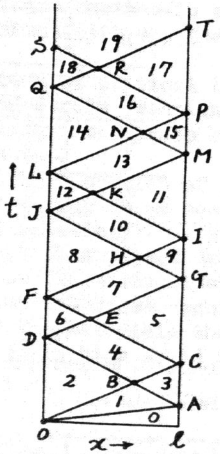

Fig.3 (x, t) diagram for high speed tension of a bar of length l of which material property is elastic-linearly work hardening.

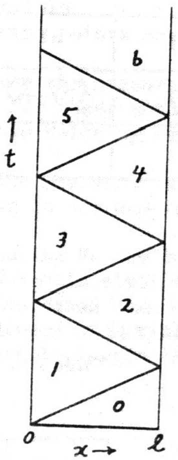

Fig.4 Special case of Fig.3. Material property is rigid-linearly work hardening.

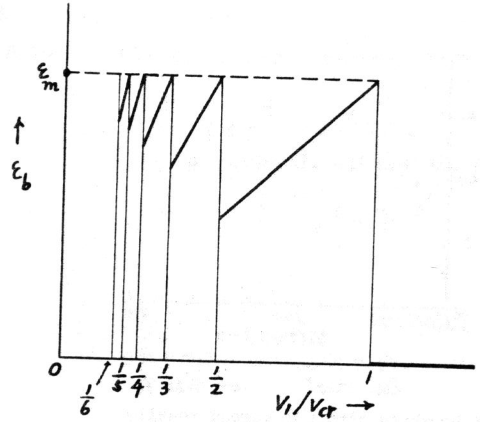

Fig.5 Theoretical relation of breaking strain ε_b versus tensile velocity V_1 in high speed tension of finite bar. Material property: rigid-linearly hardening.

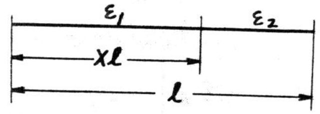

Fig.6 Strain distribution form in a specimen.

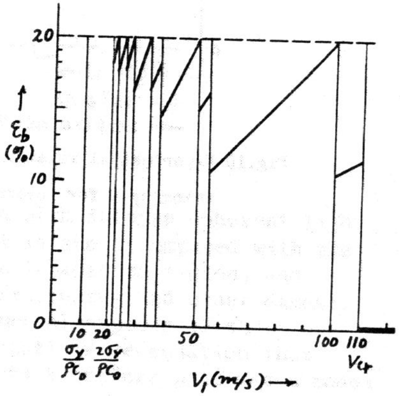

Fig.7 Theoretical relation of ε_b versus V_1 . Material property: elastic-linearly work hardening.

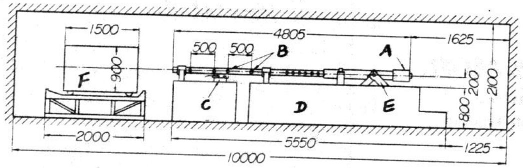

Fig.8 High speed impact loading machine.
A: gun barrel,
B: projectile velocity measuring locations, C: test piece setting part, D: concrete foundation, E: bed of gun barrel, F: sand box.

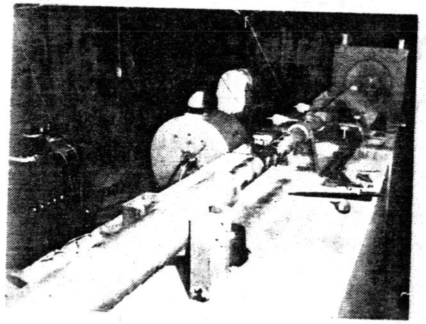

Fig.9 Photograph of testing machine & accessories.

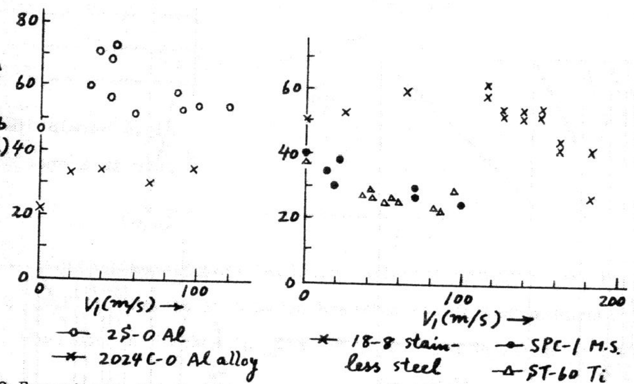

Fig.10 Experimental relation of breaking strain ε_b versus tensile velocity V_1 for several metals.

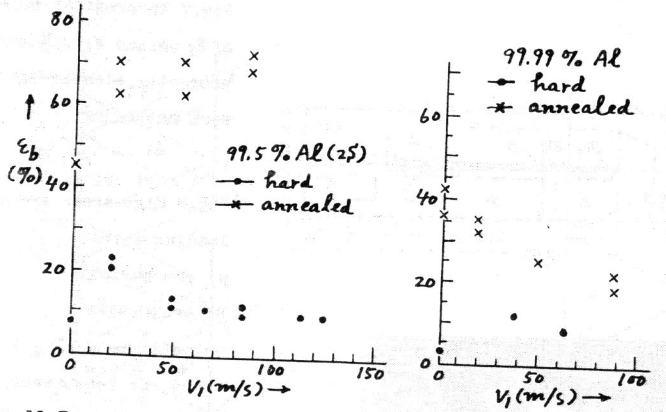

Fig.11 Experimental relation of ε_b versus V_1 for pure aluminiums.